arXiv:2211.10469v1 [cs.LG] 18 Nov 2022

Hub-VAE: Unsupervised Hub-based Regularization of Variational Autoencoders

Priya Mani* Carlotta Domeniconi†

Abstract

Exemplar-based methods rely on informative data points or prototypes to guide the optimization of learning algorithms. Such data facilitate interpretable model design and prediction. Of particular interest is the utility of exemplars in learning unsupervised deep representations. In this paper, we leverage hubs, which emerge as frequent neighbors in high-dimensional spaces, as exemplars to regularize a variational autoencoder and to learn a discriminative embedding for unsupervised down-stream tasks. We propose an unsupervised, data-driven regularization of the latent space with a mixture of hub-based priors and a hub-based contrastive loss. Experimental evaluation shows that our algorithm achieves superior cluster separability in the embedding space, and accurate data reconstruction and generation, compared to baselines and state-of-the-art techniques.
Keywords: representation learning; regularization; exemplar selection; hubness phenomenon

1 Introduction

Traditional exemplar-based machine learning methods, such as the Parzen window estimator Parzen (1962), nearest neighbor methods Cover and Hart (1967), and exemplar-SVMs Malisiewicz, Gupta, and Efros (2011), rely on a set of exemplars and on a distance metric defined on the training data to learn a predictive model. Exemplars are instances selected from the training data which are informative for a given learning task. Exemplar-based methods improve the discriminative ability of a model, and support interpretable model design and prediction. In deep learning, exemplar-based methods are typically used to explain post-training the predictions of supervised black-box models (e.g., Ribeiro, Singh, and Guestrin (2016), Guidotti et al. (2019)). Such methods are model-agnostic, as the learned exemplars do not contribute to the training of a black-box model, but are instead used to make the model interpretable. A different approach in exemplar-based deep learning (the focus of this paper) is to leverage exemplars *during* the training of a deep neural network to regularize the latent embedding (e.g., Snell, Swersky, and Zemel (2017), Norouzi, Fleet, and Norouzi (2020), Bautista et al. (2016)). In this paper, we leverage exemplars to train an unsupervised generative model, which learns discriminative latent embeddings suitable for unsupervised down-stream tasks.

Variational autoencoders (VAEs, Kingma and Welling (2014)) are a popular deep learning framework for unsupervised generative models. A VAE maps an input data point $\mathbf{x}$ into a distribution $q_\phi(\mathbf{z}|\mathbf{x})$ in the latent space (known as the *variational posterior*), through an encoder network parameterized by ϕ. The latent representation $\mathbf{z}$ is mapped into a distribution of the reconstructed input $p_\theta(\mathbf{x}|\mathbf{z})$ through a decoder network parameterized by θ. A VAE regularizes the latent embedding by modeling a prior distribution $p(\mathbf{z})$ over the latent space. The objective when training a VAE is to maximize a lower bound on the log marginal likelihood of $\mathbf{x}$, derived by variational inference:

$$\mathcal{L}(\phi,\theta;\mathbf{x}) = \mathbb{E}_{q_\phi(\mathbf{z}|\mathbf{x})}[\log p_\theta(\mathbf{x}|\mathbf{z})] - D_{\mathrm{KL}}(q_\phi(\mathbf{z}|\mathbf{x})||p_\theta(\mathbf{z})),$$

where $D_{\mathrm{KL}}(\cdot)$ is the KL-divergence between distributions.

Various approaches have been proposed in the literature to regularize the latent space of a VAE, e.g. learning a disentangled latent representation Higgins et al. (2017), Kim and Mnih (2018), and learning an informative prior distribution Norouzi, Fleet, and Norouzi (2020), Tomczak and Welling (2018). The predictive performance of a model which uses latent embeddings for an unsupervised down-stream task depends on the separability of data clusters in the latent space. In this work we propose to use *hubs* as exemplars to drive the regularization of the latent space. The hubness phenomenon Radovanovic, Nanopoulos, and Ivanovic (2010) refers to the emergence of few data points that are frequent neighbors of the data. Such phenomenon affects nearest neighbor computations and the *cluster assumption* Chapelle, Schlkopf, and Zien (2010).

To compute hubs in a collection of data, the concept of *hubness score* is used. The hubness score $N_k(\mathbf{x})$ of a data point $\mathbf{x}$ is defined as the number of points that have $\mathbf{x}$ as their k-nearest neighbor. The data points which contribute to the hubness of $\mathbf{x}$ are termed the *reverse k-nearest neighbors* of $\mathbf{x}$. A hub is a data point whose hubness score exceeds by a certain threshold the mean hubness score of the data: $N_k > \mu_{N_k} + \lambda\sigma_{N_k}$ where

*George Mason University, USA.
†George Mason University, USA.

Copyright © 2023 by SIAM
Unauthorized reproduction of this article is prohibited

μ_{N_k} and σ_{N_k} are the mean and standard deviation of the distribution of hubness scores within the data. Whether a hub has a positive or negative influence on data clustering depends on the degree of label mismatch between the hub and its reverse k-nearest neighbors. *Bad* hubs with greater than 50% label mismatch appear near cluster boundaries and can cause the merging of unrelated clusters, while *good* hubs are located near the true cluster centers, and can be useful seeds to guide data clustering Tomasev et al. (2014); Mani and Domeniconi (2020). Previous work on regularization doesn't account for hubness in their objectives.

In this paper, we regularize a VAE by leveraging good hubs as exemplars learned in the latent space. We learn a discriminative latent embedding by modeling a mixture of hub-based priors, and an adversarial margin between bad neighbors (i.e. k-nearest neighbors with a label mismatch) via contrastive learning in the latent space Schroff, Kalenichenko, and Philbin (2015).

1.1 Design Considerations Hubs exhibit characteristics which make them well-suited to be selected as exemplars to learn an embedding space for clustering. In fact, good hubs facilitate the generation of prototypes of a given class, due to their proximity to cluster centers. A recent approach called Exemplar-VAE Norouzi, Fleet, and Norouzi (2020) uses exemplars chosen at random to regularize a VAE by learning a mixture of exemplar-based priors distribution. As such, the resulting components of the prior distribution may include outliers or data points at the boundaries of clusters, which may merge clusters in the learned embedding space. Furthermore, the chosen exemplars do not depend on the evolving latent space of the VAE. In contrast, our proposed approach computes hubs in the VAE latent space which evolves with training. To further enhance the learned embeddings, Hub-VAE also optimizes a contrastive loss term that increases the margin between points and their nearest neighbors with a mismatch in estimated labels.

Fig. 1(a) shows a sample of hubs selected as exemplars by Hub-VAE from the class digit "3" (Dynamic MNIST dataset). Similarly, Fig. 1(b) shows a sample of exemplars chosen by Exemplar-VAE. In Fig. 1(b), we highlight the images which could be confused as members of another class (e.g. class 8) and those which show a large variation from the prototypical image of digit 3. The hubs chosen by Hub-VAE are closely aligned to prototypical shapes of digit 3, and have a better image quality, while the images chosen by Exemplar-VAE have a large stroke variability. In Fig. 1(c)-1(d), we show the encoding of the test data for DynamicMNIST obtained by Hub-VAE and Exemplar-VAE, respectively. As a consequence of the chosen hubs as exemplars, the clusters learned by Hub-VAE are more compact and better separated. We computed the clustering accuracy of digit 3 on the encoded embedding of test data. We used k-means to cluster the data and assigned each cluster to the majority class label in the cluster. Exemplar-VAE results in an average accuracy of 0.83 ($\pm$0.01) for digit class 3 and Hub-VAE gives an average accuracy of 0.87 ($\pm$0.06). This experiment shows the potential of a hub-based regularization of VAEs, particularly for clustering tasks which can benefit from the properties of hubs.

1.2 Contributions We present a novel approach (Hub-VAE) for the design of variational autoencoders, and leverage the hubness phenomenon to guide the regularization of the latent space via hub exemplars. This gives an embedding space well-aligned with the clustering structure of the data, which also lead to accurate data reconstruction and generation. Our main contributions are:

1. **Unsupervised regularization and hub-based priors**: We propose an unsupervised and exemplar-based regularization framework for VAEs, built on a data-driven selection of hubs in the latent space. We use a mixture of hub-based priors to regularize the VAE latent space by selecting informative hubs as exemplars.
2. **Unsupervised contrastive loss**: We further regularize the VAE latent space via an adversarial margin between data points and neighbors with mismatched estimated labels, via a contrastive loss.
3. **Improved cluster separability and generative modeling**: We empirically evaluate our method on data clustering, representation learning, and generative modeling. Our experiments show that Hub-VAE is competitive against the state-of-the-art.

2 Related Work

Variational auto-encoders are versatile, deep generative models with a wide range of applications (van den Oord, Vinyals, and Kavukcuoglu, 2017; Schönfeld et al., 2019; Gregor et al., 2019). VAEs have a strong theoretical foundation and are easier to train and optimize than other classes of generative models (Radford, Metz, and Chintala, 2016). In this section we briefly discuss previous work on VAEs.

2.1 VAE Regularization Several approaches have been proposed to learn a disentangled representation in the latent space and make the latent dimensions independent. The β-VAE (Higgins et al., 2017) weights the KL-divergence term by a factor β to trade off learning an accurate reconstruction with disentanglement,

Copyright © 2023 by SIAM
Unauthorized reproduction of this article is prohibited

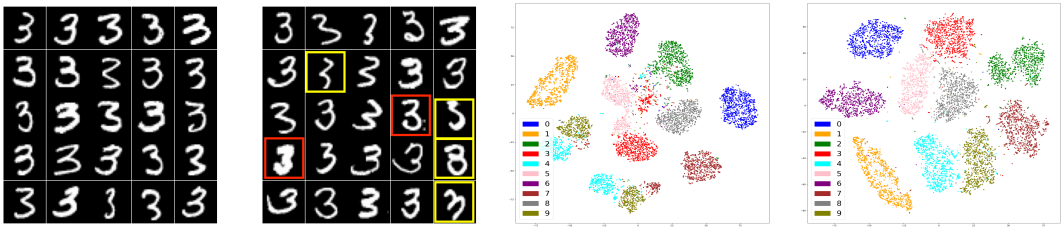

(a) (b) (c) (d)

Figure 1: A sample of digit 3 exemplars learned by (a) Hub-VAE and (b) Exemplar-VAE. Red bounding boxes indicate images with noise or defects and yellow bounding boxes indicate images that have a large stroke variation. For example, one of the highlighted images can be mistaken as a member of class 8. (c)-(d) show the TSNE plots of DynamicMNIST test data embeddings learned by (c) Hub-VAE and (d) Exemplar-VAE. The TSNE plots are color-coded according to ground-truth. The clusters obtained by Hub-VAE are more compact and better separated, which lead to a superior clustering accuracy for digit 3: 87% (Hub-VAE) vs. 83% (Exemplar-VAE).

while Factor-VAE (Kim and Mnih, 2018) encourages the representations to be factorial. Another way to learn an expressive and interpretable latent representation is to modify the prior distribution of the VAE. (Johnson et al., 2016; Hoffman and Johnson, 2016) have shown that the prior is essential to improving the performance of the VAE and several methods have proposed using a mixture of Gaussians prior. However, they do not allow for a closed-form optimization of the VAE objective. The authors in (VAE-Vampprior, (Tomczak and Welling, 2018)) learn an approximation of the optimal mixture prior as a variational mixture of posteriors based on pseudo-inputs which are learned through the VAE optimization. The recent work in (Exemplar-VAE, (Norouzi, Fleet, and Norouzi, 2020)) learns a mixture of exemplar-based priors, where the exemplars are chosen from the training data, and proposes a framework for conditional image generation. The work in (Tran, Pantic, and Deisenroth, 2021) introduces a mixture prior with a Cauchy-Schwarz divergence term to regularize the VAE. The work (ByPE-VAE, (Ai et al., 2021)) conditioned the mixture prior on a Bayesian pseudo-coreset which is learned along with the optimization of VAE.

2.2 Contrastive Learning Contrastive learning is closely related to large margin nearest neighbors (LMNN, (Weinberger, Blitzer, and Saul, 2005)) in traditional metric learning and optimizes a similar objective in a self-supervised or supervised deep-learning setting. A common approach is to select positive and negative samples with respect to an anchor data point, and to optimize the latent space so that positive samples are near each other in the learned representation, while negative samples are pushed farther away from the anchor. Several variants of contrastive losses have been proposed, such as to select positive samples by data augmentation (Chen et al., 2020), co-occurrence (Tian, Krishnan, and Isola, 2020), and to choose important triplets for learning (Bengio et al., 2009). (Li, Kan, and He, 2020) proposed an unsupervised deep metric learning method where a contrastive ratio between cluster centers is minimized.

2.3 Hubness Phenomenon Radovanovic, Nanopoulos, and Ivanovic (2010) provides a detailed theoretical study of the hubness phenomenon, its emergence, and its impact on learning tasks. Much of the previous work on hubness consider hubs as detrimental to their learning task (e.g., music retrieval (Berenzweig, 2007), finger-print identification (Hicklin, Watson, and Ulery, 2005), zero-shot learning (Zhang, Xiang, and Gong, 2017)), and aim to reduce hubness in data ((Feldbauer and Flexer, 2019)). However, few approaches have attempted to leverage hubs for unsupervised learning. (Tomasev et al., 2014) empirically analyzed the role of hubs w.r.t k-means clustering. This work identified good hubs as cluster prototypes and designed several hub-based variants of k-means to leverage hubs as cluster centroids in k-means iterations. Mani and Domeniconi (2020) identified good hubs using a pre-trained classifier and leveraged them to optimize a subspace clustering algorithm.

3 Hub-based VAE Regularization

The architecture of Hub-VAE is given in Fig. 2. The model consists of an encoder which maps data and hubs into their respective distributions in the latent space. The encoded data and hubs are reconstructed using a shared decoder. The encoder and the decoder can be viewed as parametric functions which learn the

Copyright © 2023 by SIAM
Unauthorized reproduction of this article is prohibited

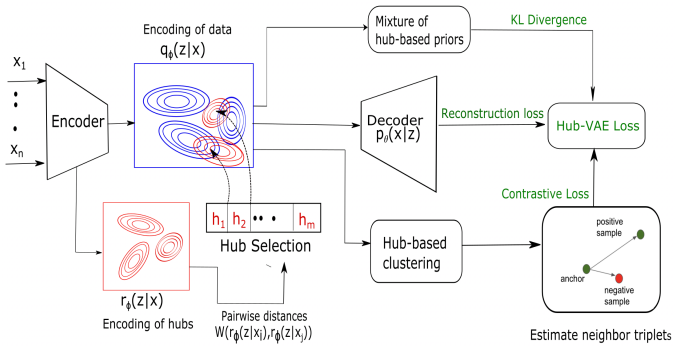

Figure 2: Hub-VAE architecture

parameters of the variational posterior and hub-based prior, and the generative model respectively.

We next formally define the components of Hub-VAE and how they are combined together. Let $\mathbf{x} = \{\mathbf{x}_i\}_{i=1}^n$ be the input data and $\mathbf{H} = \{\mathbf{x}_h\}_{h=1}^m, m < n$ be the input representation of the hubs selected from the latent embedding of $\mathbf{x}$, where m is the number of components in the hub-based prior. Each data point $\mathbf{x}_i$ is encoded into a variational posterior distribution $q_\phi(\mathbf{z}|\mathbf{x}_i) = \mathcal{N}(\mathbf{z}|\mu_\phi(\mathbf{x}_i), \Sigma_\phi(\mathbf{x}_i))$, while each hub $\mathbf{x}_h$ is encoded into a component prior distribution $r_\phi(\mathbf{z}|\mathbf{x}_h) = \mathcal{N}(\mathbf{z}|\mu_\phi(\mathbf{x}_h), \sigma^2 I)$ in the latent space, where $\mathcal{N}(.)$ denotes the Gaussian distribution, μ_ϕ and Σ_ϕ denote parametric mean and covariance functions which are learned by the encoder network with parameter set ϕ. The sampled latent space variable is mapped back into the input space through a decoder using a generative model $p_\theta(\mathbf{x}_i|\mathbf{z})$. To simplify the presentation, we denote $\mathbf{Q}_i^{(\phi)} = q_\phi(\mathbf{z}|\mathbf{x}_i)$, $\mathbf{R}_h^{(\phi)} = r_\phi(\mathbf{z}|\mathbf{x}_h)$ and $\mathbf{P}_i^{(\theta)} = p_\theta(\mathbf{x}_i|\mathbf{z})$. The encoder networks share the same parameter set ϕ. The prior distribution is defined as an isotropic Gaussian with scalar variance σ^2, while the variational posterior has a diagonal covariance Σ. The mean and variance of the variational posterior, as well as the mean of the mixture of hub-based priors are learned. The specific form of the distribution of the decoder depends on the type of data; typically a Bernoulli distribution is used for binary or discrete data and a Gaussian distribution is used for continuous data. §3.1, §3.2 and §3.3 describe each component of Hub-VAE in detail. §3.4 describes the overall objective function of Hub-VAE. The pseudocode for Hub-VAE is given in Algorithm 1 in the supplementary material.

3.1 Hub Selection We compute the hubs at the beginning of each training epoch, and use them to learn a mixture prior distribution. Hubs are computed within each mini-batch of an epoch from the k-nearest neighbor graph (k-NN) of the data, as defined in §1. A variational encoder learns data distributions instead of point estimates in the latent space. Hence, we construct the k-NN graph based on the 2-Wasserstein Givens and Shortt (1984) distance between the learned distributions in the latent space. Given two distributions $p_i(\mu_i, \mathbf{\Sigma}_i)$ and $p_j(\mu_j, \mathbf{\Sigma}_j)$ with means μ_i, μ_j, and diagonal covariances $\mathbf{\Sigma}_i$, $\mathbf{\Sigma}_j$ respectively, the 2-Wasserstein distance between the distributions is defined as $W(p_i, p_j) = (||\mu_i - \mu_j||_2^2 + ||\mathbf{\Sigma}_i^{1/2} - \mathbf{\Sigma}_j^{1/2}||_F^2)^{1/2}$ where $||.||_F$ denotes the Frobenius norm. We set $\lambda = 0.5$ and $k = \sqrt{B}$ to compute the hubness scores N_k (defined in §1), where B is the number of data points in a mini-batch.

As discussed in §1, not all hubs exhibit useful clustering properties. While *good* hubs appear near the centers of the true clusters within data, a *bad* hub has a significant label mismatch with its reverse k-nearest neighbors (RkNN), and can negatively affect tasks involving similarity or nearest neighbor computations. *A bad hub* is a hub whose label mismatches with more than 50% of its reverse k-nearest neighbors.Identifying bad hubs without access to class labels is a challenge. We address this problem by formulating a scoring function to filter bad hubs based on the characteristics exhibited by hubs in the latent space. Good hubs tend to be located near dense regions; hence the pairwise distances between the distributions of good hubs and their reverse nearest neighbors tend to be smaller then those of bad hubs. As a consequence, the average probability of reconstructing a good hub from the distribution of its reverse k-nearest neighbors is higher than for bad hubs. Based on this, we formulate a scoring function for good hubs:

$$G(\mathbf{x}_h) = \frac{\sum_{r \in \mathrm{RkNN}(\mathbf{z}_h)} p_\theta(\mathbf{x}_h|\mathbf{z}_r)}{\sum_{r \in \mathrm{RkNN}(\mathbf{z}_h)} W(q_\phi(\mathbf{z}|\mathbf{x}_r), q_\phi(\mathbf{z}|\mathbf{x}_h))},$$

where q_ϕ and p_θ denote the distributions learned by the encoder and decoder respectively; $\mathbf{x}_h$ and $\mathbf{x}_r$ denote the input representations of a hub and its reverse k-nearest neighbor; $\mathbf{z}_h$ and $\mathbf{z}_r$ denote the data points sampled in the latent space from their encoded distributions.

To motivate the choice of the scoring function above, consider the plots given in Figure 3 which show the hubs computed in an epoch and their characteristics for the datasets used in our experiments. The x-axis in each sub-plot of Figure 3 denotes normalized ($\mu_{N_k} = 0$, $\sigma_{N_k} = 1$) hubness scores. The y-axis denotes bad hubness. The bad hubness score of a hub is computed as the percentage of its RkNN with a label mismatch. For the purpose of this analysis, we use the ground truth labels to compute bad hubness.

Copyright © 2023 by SIAM
Unauthorized reproduction of this article is prohibited

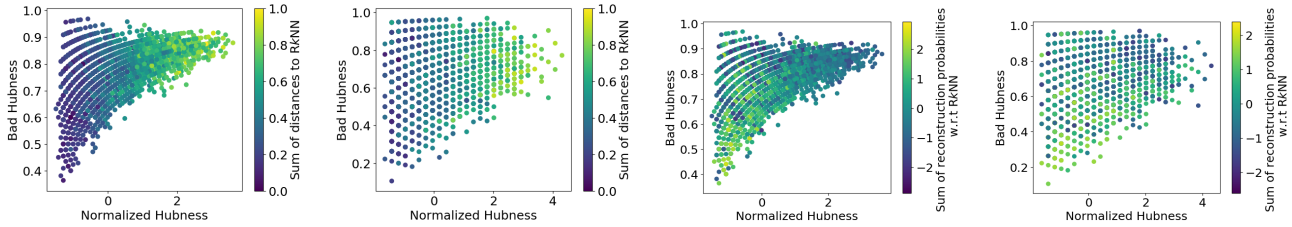

(a) Dynamic MNIST (b) Fashion MNIST (c) Dynamic MNIST (d) Fashion MNIST

Figure 3: Scatter plots of characteristics of hubs. The x-axis in each sub-plot denotes normalized ($\mu_{N_k} = 0$, $\sigma_{N_k} = 1$) hubness scores. The y-axis denotes bad hubness. The hubs are color-coded by the sum of the pairwise distances to their reverse k-nearest neighbors (RkNN) in plots (a)-(b), and by their reconstruction probabilities w.r.t. the distributions of their RkNN in plots (c)-(d). Hubs with high pairwise distances (top-right quadrant of (a)-(b)) and low reconstruction probabilities (bottom-left quadrant of (c)-(d)) with respect to their RkNN are strong bad hubs.

The hubs are color-coded by the sum of the pairwise distances to their RkNN in plots (a)-(d), and by their reconstruction probabilities w.r.t. the distributions of their RkNN in plots (e)-(h). We can see that the hubs with high pairwise distances (top-right quadrant of (a)-(d)) and low reconstruction probabilities (bottom-left quadrant of (e)-(h)) with respect to their reverse k-nearest neighbors are strong bad hubs.The above characteristics exhibited by hubs in the latent space of VAE, motivate the coice of the scoring function $G(\mathbf{x}_h)$ above. We use a threshold to select good hubs based on $G(\mathbf{x}_h)$, setting the threshold adaptively to $\frac{\max(z\text{-score}(G))}{2}$.

Prior to each training epoch, we pre-compute a pool of good hubs by selecting them from each mini-batch in the epoch. The data in each mini-batch of an epoch are encoded into the latent space using the configuration of the VAE model trained in the previous epoch. The training of the VAE in the current epoch is then carried out, and uses the selected pool of hubs to regularize the latent space.

3.2 Hub-based Prior Distribution We learn a mixture of *good* hub-based priors to regularize the VAE. Each mini-batch in a training epoch samples a subset of hubs from the selected pool of hubs for that epoch. We define the component prior distribution corresponding to each hub as an isotropic Gaussian with a mean function which depends on the chosen hub and shared covariance among all of the hub distributions, as also done in previous work on exemplar based priors Norouzi, Fleet, and Norouzi (2020); Tomczak and Welling (2018): $\mathbf{R}_h^{(\phi)} = r_\phi(\mathbf{z}|\mathbf{x}_h) = \mathcal{N}(\mathbf{z}|\mu_\phi(\mathbf{x}_h), \sigma^2 I)$, where σ is a scalar. Based on these distributions, we define the KL-divergence loss between the variational posterior and the hub-based prior as $\mathcal{L}_{\text{KL}}(\mathbf{x}_i, \phi) = D_{\text{KL}}(\mathbf{Q}_i^{(\phi)} || \frac{1}{m}\sum_{j=1}^{m} \mathbf{R}_{h_j}^{(\phi)})$. The reconstruction loss component of the VAE objective $\mathcal{L}_R(\mathbf{x}_i, \phi, \theta) = -\mathbb{E}_{\mathbf{Q}_i^{(\phi)}}[\log \mathbf{P}_i^{(\theta)}]$ further regularizes the latent space. The complete loss function for Hub-VAE is given in § 3.4. In Hub-VAE a hub is chosen from the selected pool of hubs in the latent space, and is encoded into a latent representation using the hub-based prior. The decoder then reconstructs the latent representation as a new sample. For generative modeling, Hub-VAE requires the decoder network as well as the learned pool of hubs and the hub-based prior r_ϕ.

3.3 Hub-based Contrastive Learning We regularize the VAE to learn a discriminative latent space embedding by increasing the margin between a point and its neighbor when a label mismatch is detected. This regularization is useful in high-dimensional latent spaces which are affected by the emergence of bad hubs. We achieve this through contrastive learning within the k-neighborhood of each point. Contrastive learning works similarly to the hinge loss in Weinberger, Blitzer, and Saul (2005). Positive and negative samples are selected w.r.t an anchor point, depending on the label match/mismatch between the anchor and the samples. The distances between each triplet (anchor, positive, and negative sample) are adjusted such that the distance of the anchor to the negative sample is larger than that of the positive sample by a certain margin.

Contrastive learning is typically applied in a supervised setting where the class labels of data points are known. Our model is unsupervised which brings forth the challenging problem of selecting good and bad neighbors without access to their labels. To overcome this issue, we cluster the data in the latent space and

Copyright © 2023 by SIAM
Unauthorized reproduction of this article is prohibited

use the clustering labels as a proxy for the ground truth. Since good hubs appear near cluster centers, we seed the clustering process using the hub sample to obtain a higher clustering quality. In each mini-batch, the hubs are clustered using k-means[1], and the rest of the data are assigned to the cluster label of its nearest hub, as computed by the 2-Wasserstein distance between their distributions.

Given the cluster labels, we choose triplets from the neighborhood of each data point as follows: each data point is an anchor, the farthest neighbor that shares the same cluster label with the anchor is chosen as the positive sample, and the neighbors with label mismatch are chosen as the negative samples. The contrastive loss of a given anchor point $\mathbf{x}_a$ with t triplets $(\mathbf{x}_a, \mathbf{x}_p, \mathbf{x}_{n_i}), i = 1, 2, \ldots t$ is defined as:

$$\mathcal{L}_C(\mathbf{x}_a, \phi) = \sum_{i=1}^{t} [W(\mathbf{Q}_a^{(\phi)}, \mathbf{Q}_p^{(\phi)}) - W(\mathbf{Q}_a^{(\phi)}, \mathbf{Q}_{n_i}^{(\phi)}) + 1]_+$$
$$\{\mathbf{x}_p, \mathbf{x}_{n_i}\} \in k\mathrm{NN}(\mathbf{x}_a), i = 1, 2, \ldots\ldots t$$
$$l(\mathbf{x}_a) \neq l(\mathbf{x}_{n_i}), l(\mathbf{x}_a) = l(\mathbf{x}_p)$$

where $\mathbf{x}_p$ is the positive sample, $\mathbf{x}_{n_i}$ are negative samples associated with the anchor, and $l(\mathbf{x})$ is the label of $\mathbf{x}$. The loss is minimized when the distance from the anchor to each negative example is greater then the distance to the positive example by 1. Hence, training using this loss makes the anchor (i.e. its embedding) significantly closer to the positive example than to negative examples[2].

A training mini-batch is a sample of data points, and the distribution of cluster densities in the sample could vary. Hence we compute adaptive neighbors for each data point to reduce over-stepping cluster boundaries due to the selection of k nearest neighbors. We select triplets from an adaptive neighborhood of each data point in the latent space. The adaptive neighbors are computed as follows: we construct a k-nearest neighbor graph and compute mean μ_D and standard deviation σ_D of the distribution of kth-neighbor distances across the data points, and eliminate the neighbors whose distances exceed $\mu_D + 2\sigma_D$. The hub seeded clustering together with the adaptive neighborhood facilitates selection of more accurate triplets for contrastive learning.

3.4 Hub-VAE Objective Function

The objective function minimized by Hub-VAE is given below. It includes the following terms: (1) the reconstruction loss between the data point given in input to the encoder and the output of the decoder; (2) the KL-divergence between the variational posterior and the hub-based prior; (3) the contrastive loss within the neighborhood of the input data point.

$$L_{\text{HUB-VAE}}(\mathbf{x}_a; \phi, \theta) =$$
$$\mathcal{L}_R(\mathbf{x}_a, \phi, \theta) + \mathcal{L}_C(\mathbf{x}_a, \phi) + \beta \mathcal{L}_{\mathrm{KL}}(\mathbf{x}_a, \phi)$$

The training of Hub-VAE is conducted in mini-batches, and each mini-batch minimizes $L_{\text{HUB-VAE}}$ over the data points in that mini-batch. The reparameterization Kingma and Welling (2014) is applied to $q_\phi(\mathbf{z}|\mathbf{x}_a)$ to enable back-propagation through the encoder. Hub-VAE performs stochastic optimization using the Adam algorithm Kingma and Ba (2015) with normalized gradients Yu et al. (2017). Training is performed for 100 epochs and a validation loss is computed at the end of each epoch using the current model configuration and a separate validation data. Similarly to previous models proposed in the literature Norouzi, Fleet, and Norouzi (2020); Tomczak and Welling (2018), the validation loss uses all of the learned hubs as exemplars and does not incorporate the contrastive loss term in its objective[3]

$$L_{\mathrm{val}}(\mathbf{x}_v; \phi, \theta) = \mathcal{L}_R(\mathbf{x}_v, \phi) + \beta D_{\mathrm{KL}}(\mathbf{Q}_v^{(\phi)} || \frac{1}{|\mathcal{H}|} \sum_{j=1}^{|\mathcal{H}|} \mathbf{R}_j^{(\phi)})$$

where $\mathcal{H}$ is the pool of selected good hubs and $\mathbf{x}^v$ is a validation instance. The configuration which results in the minimum validation loss is used as the final model.

4 Experiments

We compare the methods on four well-known benchmark datasets: Dynamic MNIST (DMNIST) Salakhutdinov and Murray (2008), Fashion MNIST (FMNIST) Xiao, Rasul, and Vollgraf (2017), USPS[4], and Caltech101Silhouettes[5] (Caltech101). We evaluate Hub-VAE against a baseline standard-VAE with a factored Gaussian distribution which is compared in Tomczak and Welling (2018), and state-of-the-art VAE regularization methods which modify the prior distribution: ByPE-VAE Ai et al. (2021), Exemplar-VAE Norouzi, Fleet, and Norouzi (2020), denoted as Ex-VAE, and VAE-Vampprior Tomczak and Welling (2018). For all

[1] Number of clusters in k-means is set to the number of classes.

[2] Since we use cluster labels to choose $\mathbf{x}_p$ and $\mathbf{x}_{n_i}$, each anchor $\mathbf{x}_a$ will have a positive sample within its neighborhood. When $\{\mathbf{x}_{n_i}\}$ is an empty set, $\mathcal{L}_C(\mathbf{x}_a, \phi) = 0$.

[3] $\mathcal{L}_C$ isn't included in the validation objective as its computation requires knowledge of the number of classes in the data. Furthermore, $\mathcal{L}_C$ acts as an additional regularizer, and the learning of VAE can be approximated by L_{val}, without sacrificing model performance.

[4] `https://pytorch.org/vision/stable/datasets.html`

[5] `https://people.cs.umass.edu/~marlin/data/caltech101_silhouettes_28_split1.mat`.

Copyright © 2023 by SIAM
Unauthorized reproduction of this article is prohibited

Data	VAE-Gaussian	VAE-Vamp	Ex-VAE	ByPE-VAE	Hub-VAE
DMNIST	0.52 (0.02)	0.58 (0.01)	0.64 (0.01)	0.66 (0.01)	**0.73** (0.02)
USPS	0.52 (0.01)	0.64 (0.01)	0.69 (0.01)	0.68 (0.01)	**0.76** (0.01)
FMNIST	0.57 (0.01)	0.58 (0.01)	0.59 (0.01)	0.61 (0.01)	**0.64** (0.01)
Caltech101	0.59 (0.002)	0.60 (0.002)	0.60 (0.002)	**0.61** (0.001)	0.60 (0.004)

Table 1: k-means V-measure. We show mean (std) over 10 runs. Statistically significant results are underlined.

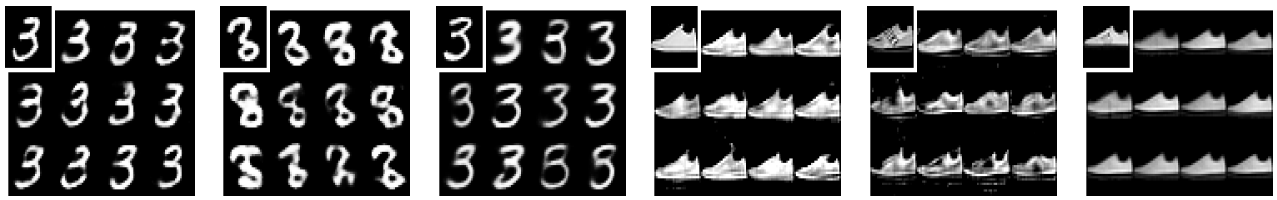

(a) Hub-VAE (b) Exemplar-VAE (c) ByPE-VAE (d) Hub-VAE (e) Exemplar-VAE (f) ByPE-VAE

Figure 4: Conditional image generation from classes 3 in DMNIST and 'Sneaker' in FMNIST. The inset shows reference images.

experiments, we set the number of components $m = 1000$ in the prior distribution, and the latent space dimensionality $d = 40$ [6]. All methods are run for a maximum of 100 epochs. We use early-stopping with a look-ahead of 50 epochs. The initial value of β in $L_{\text{HUB-VAE}}$ is set to 1 and is annealed as the epochs progress. Results are shown on average over 10 runs and statistical significant results are underlined. All experiments are run on a A100 GPU on the Google Cloud Platform. Hub-VAE takes on average 28 sec to run an epoch for DMNIST, 37 sec for FMNIST, and 5 sec for USPS and Caltech101. Dataset summary and comparison of running times across all methods are given in the supplementary material.

4.1 Representation Learning We evaluate the efficacy of the learned latent embeddings for unsupervised tasks using the V-measure Rosenberg and Hirschberg (2007) and KNN purity. The V-measure is an entropy-based evaluation metric computed as the harmonic mean of homogeneity and completeness score of a given clustering. Homogeneity measures the degree to which the members of a cluster belong to the same class, while the completeness score measures the degree to which the members of a class belong to the same cluster. KNN purity measures the % of k-nearest neighbors which share the same class label, i.e. the degree to which the cluster assumption holds on a given test data. The number of classes for k-means clustering is set equal to the true number of classes in the data.

Tables 1 show the results on V-measure. The results for KNN purity are given in the supplementary material. Hub-VAE outperforms baselines by at least 8% for V-measure on DMNIST, FMNIST, and USPS, and attains comparable performance on Caltech101. Hub-VAE further achieves superior performance in V-Measure compared to Ex-VAE and ByPE-VAE for the large majority of the datasets, thus showing the advantage of using hubs as exemplars to improve cluster separability in the embedding space. We provide an ablation study, t-SNE plots, and additional results on CIFAR-10 data in the supplementary material.

4.2 Reconstruction and Generation In Fig. 4, we compare the quality of exemplar-based generative modeling using conditional image generation on Hub-VAE, Exemplar-VAE, and ByPE-VAE. We depict generated images from class 3 for DMNIST and from class 'Sneaker' for FMNIST. We observe that some of the images generated by Exemplar-VAE and ByPE-VAE resemble digits 8 or 5. These classes exhibit features which can confound their members, and they are embedded in close proximity in the latent space learned by Exemplar-VAE and ByPE-VAE. In contrast, Hub-VAE results in accurate generations and closely follow the shape of the reference image (shown in the inset). Hub-VAE separates digits with varied strokes within a class into separate clusters, which helps obtain more accurate reconstructions and generations. Similarly, Exemplar-VAE does not fully capture the shape of 'Sneaker' and also generates blurred images. The above results show that

[6] Number of coresets in ByPE-VAE, and the number of pseudo-inputs in VAE-Vampprior are set to 1000 for fair comparison.

Copyright © 2023 by SIAM
Unauthorized reproduction of this article is prohibited

Data	Hub-VAE	Ex-VAE	ByPE-VAE
DMNIST	**8.45** (0.2)	9.49 (0.6)	21.39 (0.6)
USPS	**16.44** (0.3)	20.12 (11)	37.80 (2.6)
FMNIST	25.25 (0.2)	**25.15** (0.3)	54.90 (0.6)
Caltech101	91.45 (0.6)	**87.01** (2.2)	124 (3.1)

Table 2: FID on reconstructed images. Lower values signify higher quality. Statistically significant results are underlined.

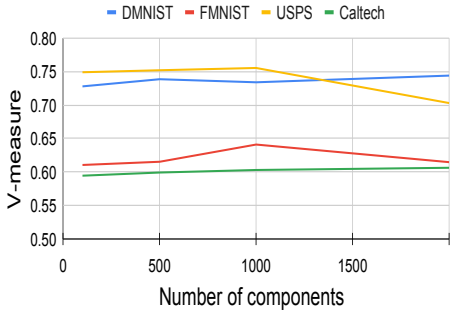

Figure 5: Sensitivity analysis on number of components.

a hub-based regularization of VAEs is useful to improve the quality of the generative modeling.

We compute Fretchet Inception Distance (FID) Heusel et al. (2017) between original and reconstructed images to evaluate their quality. In Table 2, we observe that Hub-VAE has higher reconstruction quality than its competitors for DMNIST and USPS and similar quality for FMNIST.

5 Sensitivity Analysis

We conduct sensitivity analysis to assess the influence of the number of components of the mixture prior distribution on VAE regularization. Figure 5 shows the values of k-means V-measure across different number of components $m \in \{100, 500, 1000, 2000\}$. While we see a notable increase in V-measure for FMNIST when m is increased from 500 to 1000, the trend is stable for the other datasets for this range of m values.

6 Conclusion

We proposed a data-driven, hub-based regularization approach for VAEs to learn a discriminative and interpretable latent embedding using a mixture of hub based priors and leveraging the useful clustering properties of hubs. We further enhanced the regularization by introducing a hub-based contrastive loss to increase the margin between bad neighbors in the latent space. Our method achieves competitive results against state-of-the-art VAE regularization methods.

References

Ai, Q.; HE, L.; LIU, S.; and Xu, Z. 2021. ByPE-VAE: Bayesian Pseudocoresets Exemplar VAE. In *NeurIPS 2021*.

Bautista, M. Á.; Sanakoyeu, A.; Tikhoncheva, E.; and Ommer, B. 2016. CliqueCNN: Deep Unsupervised Exemplar Learning. In *NeurIPS*.

Bengio, Y.; Louradour, J.; Collobert, R.; and Weston, J. 2009. Curriculum learning. In *ICML 2009*.

Berenzweig, A. 2007. *Anchors and Hubs in Audio-based Music Similarity*. Ph.D. thesis, Columbia University.

Chapelle, O.; Schlkopf, B.; and Zien, A. 2010. *Semi-Supervised Learning*. The MIT Press, 1st edition.

Chen, T.; Kornblith, S.; Norouzi, M.; and Hinton, G. E. 2020. A Simple Framework for Contrastive Learning of Visual Representations. In *ICML 2020*.

Cover, T. M.; and Hart, P. E. 1967. Nearest neighbor pattern classification. *IEEE Trans. Inf. Theory*, 13(1): 21–27.

Feldbauer, R.; and Flexer, A. 2019. A comprehensive empirical comparison of hubness reduction in high-dimensional spaces. *Knowl. Inf. Syst.*, 59(1): 137–166.

Givens, C. R.; and Shortt, R. M. 1984. A class of wasserstein metrics for probability distributions. *The Michigan Mathematical Journal*, 31(2): 231–240.

Gregor, K.; Papamakarios, G.; Besse, F.; Buesing, L.; and Weber, T. 2019. Temporal Difference Variational Auto-Encoder. In *ICLR 2019*.

Guidotti, R.; Monreale, A.; Matwin, S.; and Pedreschi, D. 2019. Black Box Explanation by Learning Image Exemplars in the Latent Feature Space. In *ECML PKDD 2019*.

Heusel, M.; Ramsauer, H.; Unterthiner, T.; Nessler, B.; and Hochreiter, S. 2017. GANs Trained by a Two Time-Scale Update Rule Converge to a Local Nash Equilibrium. In *NeurIPS*, volume 30.

Hicklin, A.; Watson, C.; and Ulery, B. 2005. The myth of goats: How many people have fingerprints that are hard to match. *Internal Report 7271, National Institute of Standards and Technology (NIST)*.

Copyright © 2023 by SIAM
Unauthorized reproduction of this article is prohibited

Higgins, I.; Matthey, L.; Pal, A.; Burgess, C.; Glorot, X.; Botvinick, M.; Mohamed, S.; and Lerchner, A. 2017. beta-VAE: Learning Basic Visual Concepts with a Constrained Variational Framework. In *ICLR*.

Hoffman, M. D.; and Johnson, M. J. 2016. Elbosurgery: Yet another way to carve up the variational evidence lower bound. In *Workshop in Advances in Approximate Bayesian Inference, NIPS*.

Johnson, M. J.; Duvenaud, D.; Wiltschko, A. B.; Adams, R. P.; and Datta, S. R. 2016. Composing graphical models with neural networks for structured representations and fast inference. In *NeurIPS 2016*, 2946–2954.

Kim, H.; and Mnih, A. 2018. Disentangling by Factorising. In *ICML 2018*, 2649–2658.

Kingma, D. P.; and Ba, J. 2015. Adam: A Method for Stochastic Optimization. In *ICLR*.

Kingma, D. P.; and Welling, M. 2014. Auto-Encoding Variational Bayes. In *ICLR*.

Li, Y.; Kan, S.; and He, Z. 2020. Unsupervised Deep Metric Learning with Transformed Attention Consistency and Contrastive Clustering Loss. In *ECCV 2020*.

Malisiewicz, T.; Gupta, A.; and Efros, A. A. 2011. Ensemble of exemplar-SVMs for object detection and beyond. In *ICCV 2011*, 89–96.

Mani, P.; and Domeniconi, C. 2020. Hub-based subspace clustering. *Neurocomputing*, 413: 193–209.

Norouzi, S.; Fleet, D. J.; and Norouzi, M. 2020. Exemplar VAE: Linking Generative Models, Nearest Neighbor Retrieval, and Data Augmentation. In *NeurIPS 2020*.

Parzen, E. 1962. *On estimation of a probability density function and mode*. Annals of Mathematical Statistics.

Radford, A.; Metz, L.; and Chintala, S. 2016. Unsupervised Representation Learning with Deep Convolutional Generative Adversarial Networks. In Bengio, Y.; and LeCun, Y., eds., *ICLR 2016*.

Radovanovic, M.; Nanopoulos, A.; and Ivanovic, M. 2010. Hubs in Space: Popular Nearest Neighbors in High-Dimensional Data. *J. Mach. Learn. Res.*, 11: 2487–2531.

Ribeiro, M. T.; Singh, S.; and Guestrin, C. 2016. "Why Should I Trust You?": Explaining the Predictions of Any Classifier. In *ACM SIGKDD*, 1135–1144.

Rosenberg, A.; and Hirschberg, J. 2007. V-Measure: A Conditional Entropy-Based External Cluster Evaluation Measure. In Eisner, J., ed., *EMNLP-CoNLL 2007*, 410–420.

Salakhutdinov, R.; and Murray, I. 2008. On the quantitative analysis of deep belief networks. In *ICML 2008*.

Schönfeld, E.; Ebrahimi, S.; Sinha, S.; Darrell, T.; and Akata, Z. 2019. Generalized Zero- and Few-Shot Learning via Aligned Variational Autoencoders. In *CVPR 2019*, 8247–8255.

Schroff, F.; Kalenichenko, D.; and Philbin, J. 2015. FaceNet: A unified embedding for face recognition and clustering. In *CVPR 2015*, 815–823.

Snell, J.; Swersky, K.; and Zemel, R. S. 2017. Prototypical Networks for Few-shot Learning. In *NeurIPS*, 4077–4087.

Tian, Y.; Krishnan, D.; and Isola, P. 2020. Contrastive Multiview Coding. In *ECCV 2020*. Springer.

Tomasev, N.; Radovanovic, M.; Mladenic, M.; and Ivanovic, M. 2014. The Role of Hubness in Clustering High-Dimensional Data. *IEEE Trans. Knowl. Data Eng.*, 26(3): 739–751.

Tomczak, J. M.; and Welling, M. 2018. VAE with a VampPrior. In *AISTATS 2018, Playa Blanca, Lanzarote, Canary Islands, Spain*.

Tran, L.; Pantic, M.; and Deisenroth, M. P. 2021. Cauchy-Schwarz Regularized Autoencoder. *CoRR*, abs/2101.02149.

van den Oord, A.; Vinyals, O.; and Kavukcuoglu, K. 2017. Neural Discrete Representation Learning. In *NeurIPS*, 6306–6315.

Weinberger, K. Q.; Blitzer, J.; and Saul, L. K. 2005. Distance Metric Learning for Large Margin Nearest Neighbor Classification. In *Advances in Neural Information Processing Systems 2005*, 1473–1480.

Xiao, H.; Rasul, K.; and Vollgraf, R. 2017. Fashion-MNIST: a Novel Image Dataset for Benchmarking Machine Learning Algorithms. *CoRR*, abs/1708.07747.

Yu, A. W.; Lin, Q.; Salakhutdinov, R.; and Carbonell, J. G. 2017. Normalized Gradient with Adaptive Stepsize Method for Deep Neural Network Training. *CoRR*, abs/1707.04822.

Zhang, L.; Xiang, T.; and Gong, S. 2017. Learning a Deep Embedding Model for Zero-Shot Learning. In *CVPR 2017*.

Copyright © 2023 by SIAM
Unauthorized reproduction of this article is prohibited

arXiv:2211.10469v1 [cs.LG] 18 Nov 2022

Hub-VAE: Unsupervised Hub-based Regularization of Variational Autoencoders Supplementary Material

Priya Mani* Carlotta Domeniconi†

1 Algorithm

Algorithm 1 shows the pseudo-code of training epoch for Hub-VAE.

2 Additional Experiments

Data Table 1 gives the summary statistics for the data. We evaluated our method on an additional dataset, CIFAR-10 [1].

2.1 Representation Learning We evaluate k-NN purity of data in Table 2. The value of k for computing the KNN purity is set to $k = \sqrt{n_{\text{test}}}$, where n_{test} is the number of instances in the test data. Hub-VAE outperforms baselines by at least 1% for KNN purity on DMNIST, FMNIST, and USPS, and attains comparable performance on Caltech101.

Fig. 1 shows the t-SNE plot of test data of DMNIST for ByPE-VAE. Similar to Exemplar-VAE, ByPE-VAE does not form compact clusters.

In Table 3, we evaluate k-means V-measure and KNN purity for CIFAR-10 across 5 independent training runs. We trained each method for 500 epochs for CIFAR-10. Hub-VAE outperforms the baseline and has nearly similar performance to ByPE-VAE.

2.2 Ablation Study We evaluate the influence of different components of Hub-VAE on its objective function. We compute k-means V-measure and KNN purity for our model without applying contrastive loss (Hub-VAE-NoContrastive), and without applying hub selection (Hub-VAE-NoSelection). Table 4 and Table 5show the k-means V-measure and KNN purity for these variants.

USPS and FMNIST show a significant decrease in performance for HuB-VAE variants. The performance drop is more pronounced for Hub-VAE-NoContrastive, which suggests that contrastive learning is useful in learning the underlying clustering structure of data by separating bad neighbors in the data. Hub-VAE-NoSelection results in lower V-measure and KNN purity

*George Mason University, USA.
†George Mason University, USA.
[1] https://www.cs.toronto.edu/ kriz/cifar.html

Algorithm 1 Hub-VAE

input: Data $\mathbf{x} = \{\mathbf{x}_i\}_{i=1}^n$, number of components in the prior m, # epochs =100, mini-batch size $B = 100$, $\beta = 1$, variance of prior distribution σ^2, the number of clusters K, learned hubs $\mathcal{H}$
output: Learned parameters ϕ, θ, τ
Initialize parameters ϕ, θ, τ
for each training epoch **do**
  for each mini-batch $\{\mathbf{x}_i\}_{i=1}^B$ in the epoch **do**
    Compute distributions $\mathbf{R}_i^{(\phi)}$ and $\mathbf{P}_i^{(\theta)}$ for each $\mathbf{x}_i$ in the batch
    // Compute pairwise 2-Wasserstein distances for all points in the batch
    $d_{ij} \leftarrow W(\mathbf{R}_i^{(\phi)}, \mathbf{R}_j^{(\phi)}), i, j \in [B]$
    // Compute hubs
    $\mathcal{H} \leftarrow \{\mathbf{x}_h \mid N_{\sqrt{B}}(\mathbf{x}_h) > \mu + 0.5\sigma\}$
    // Estimate good hubness score
    $G(\mathbf{x}_h) \leftarrow \frac{\sum_{r \in \text{RkNN}(\mathbf{z}_h)} p_\theta(\mathbf{x}_h|\mathbf{z}_r)}{\sum_{r \in \text{RkNN}(\mathbf{z}_h)} d_{rh}}$ for $h \in \mathcal{H}$
  end for
  Eliminate bad hubs $\mathbf{x}_{h_j}$ from the pool $\{\mathbf{x}_h\}$:
  $\mathcal{H} \leftarrow \{h \in \mathcal{H} \mid z\text{-score}(G(\mathbf{x}_h)) < \frac{\max(z\text{-score}(G))}{2}\}$
  for each mini-batch $\{\mathbf{x}_i\}_{i=1}^B$ in epoch **do**
    Compute distribution $\mathbf{Q}_i^{(\phi)}$ for each $\mathbf{x}_i$ in the batch
    Let $h_1, \ldots, h_m$ be a uniformly random sample from $\mathcal{H}$
    Let $l(\mathbf{x}_{h_j})$ be the label after using K-Means clustering on the hubs $\mathbf{x}_{h_1}, \ldots, \mathbf{x}_{h_m}$, where K denotes the number of clusters in the data
    // Assign clustering labels $\{l_i\}$ to the closest hub
    For each $i \in [B]$, let $l(\mathbf{x}_i) \leftarrow l(\mathbf{x}_{h_j})$, where $j \leftarrow argmin_j \tilde{d}_{ih_j}$, where $\tilde{d}_{ih_j} = W(\mathbf{Q}_i^{(\phi)}, \mathbf{R}_{h_j}^{(\phi)})$
    For each $a \in [B]$, compute the contrastive loss $\mathcal{L}_C(\mathbf{x}_a, \phi)$
    Compute distribution $\mathbf{P}_a^{(\theta)}$ for all $a \in [B]$
    Compute the loss $L_{\text{HUB-VAE}}(\mathbf{x}_a; \phi, \theta, \tau)$
    Back-propagate and update parameters (ϕ, θ, τ) to minimize $L_{\text{HUB-VAE}}(\mathbf{x}_a; \phi, \theta, \tau)$
  end for
end for

Copyright © 2023 by SIAM
Unauthorized reproduction of this article is prohibited

Data	# instances	# input features	# classes
DMNIST	70000	784	10
FMNIST	70000	784	10
USPS	9298	256	10
Caltech101	8671	784	101
CIFAR-10	60000	3072	10

Table 1: Dataset information

Data	VAE-Gaussian	VAE-Vamp	Ex-VAE	ByPE-VAE	Hub-VAE
DMNIST	72.77 (0.83)	86.18 (0.12)	88.24 (0.44)	**90.09** (0.42)	89.36 (0.97)
USPS	71.17 (0.68)	80.94 (0.28)	84.02 (0.59)	81.33 (0.19)	**85.79** (0.57)
FMNIST	69.71 (0.19)	71.55 (0.06)	71.69 (0.10)	71.37 (0.22)	**72.92** (0.15)
Caltech101	41.80 (0.06)	41.89 (0.08)	42.16 (0.07)	**42.52** (0.08)	42.20 (0.11)

Table 2: KNN Purity. We show mean (std) over 10 runs. Statistically significant results are underlined.

Metric	VAE-Gaussian	VAE-Vamp	Ex-VAE	ByPE-VAE	Hub-VAE
k-means V-measure	0.11 (0.002)	0.10 (0.001)	0.10 (0.004)	**0.12** (0.004)	0.11 (0.001)
KNN Purity	21.65 (0.07)	22.15 (0.05)	21.9 (0.06)	**22.71** (0.16)	22.05 (0.04)

Table 3: Evaluation of representation quality of CIFAR-10 embeddings. We show mean (std) over 5 runs. Statistically significant results are underlined.

than Hub-VAE, which shows that use of good hubs as exemplars in the mixture prior plays a significant role in learning the clustering structure of data. DMNIST and Caltech101 did not show much change in performance on the variants. A lack of decrease in performance of Hub-NoSelection compared to Hub-VAE indicates that DMNIST and Caltech101 have fewer strong bad hubs in the data which can negatively influence the neighbor computation and regularization. The lack of performance drop without contrastive learning (Hub-VAE-NoContrastive) further indicates that these datasets have relatively fewer bad neighbors than FMNIST and USPS.

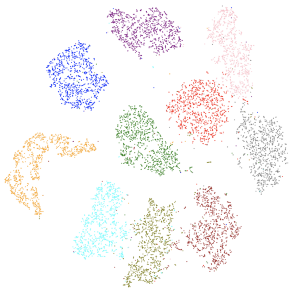

Figure 1: t-SNE plot of DMNIST test data for ByPE-VAE.

2.3 Reconstruction and Generation In Fig. 2, we compare the reconstruction of images in DMNIST for each method. The images are chosen through a random sampling of the latent space. Fig. 2(a) and (e) shows the original training images for the data being reconstructed, and (b)-(d), (f)-(h) show the reconstructions obtained by the different methods. We observe that Hub-VAE reconstructed images are less blurred and have fewer inaccuracies compared to its competitors.

The reconstructions for FMNIST in Fig. 3 show an overall lesser variability among Hub-VAE and Ex-VAE. However, it can be observed that ByPE-VAE results in blurred images and fails to capture the finer details of the images which were captured by Hub-VAE and Ex-VAE (for example, class 'Sneaker', 'Ankle boots'). Similar results can be observed for USPS, where ByPE-VAE incorrectly reconstructs digit 8 instead of digit 3, as shown by red bounding box in Fig. 4.

In Fig. 5, we compare the quality of conditional image generation on Hub-VAE and Ex-VAE.We plot the classes 'Sandals', 'Bag', 'Ankle Boots' and 'Shirt' for Fashion-MNIST. The classes 'Sandals' and 'Ankle Boots' can be confused with each other. We again

Copyright © 2023 by SIAM
Unauthorized reproduction of this article is prohibited

Data	Hub-VAE -NoSelection	Hub-VAE -NoContrastive	Hub-VAE
DMNIST	0.73 (0.02)	0.73 (0.002)	0.73 (0.02)
USPS	0.73 (0.01)	0.68 (0.01)	**0.76** (0.01)
FMNIST	0.62 (0.01)	0.60 (0.005)	**0.64** (0.01)
Caltech101	0.60 (0.001)	0.60 (0.004)	0.60 (0.004)

Table 4: k-means V-measure on Hub-VAE variants. We show mean (std) over 10 runs. Statistically significant results are underlined.

Data	Hub-VAE -NoSelection	Hub-VAE -NoContrastive	Hub-VAE
DMNIST	89.07 (0.02)	**90.36** (0.002)	89.36 (0.97)
USPS	84.17 (0.46)	83.92 (0.45)	**85.79** (0.57)
FMNIST	72.30 (0.14)	71.83 (0.0)	**72.92** (0.15)
Caltech101	41.97 (0.03)	**42.28** (0.0)	42.20 (0.11)

Table 5: KNN purity on Hub-VAE variants. We show mean (std) over 10 runs. Statistically significant results are underlined.

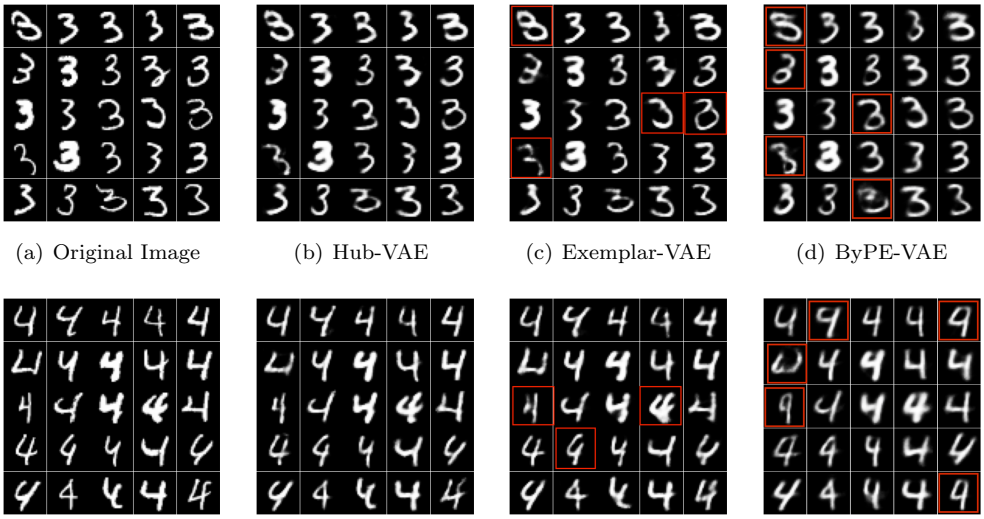

(a) Original Image (b) Hub-VAE (c) Exemplar-VAE (d) ByPE-VAE

(e) Original Image (f) Hub-VAE (g) Exemplar-VAE (h) ByPE-VAE

Figure 2: Reconstruction of randomly sampled images of digits 3 and 4 of Dynamic MNIST. (a) shows the original images of the reconstructed data. Red bounding boxes show inaccurate reconstructions of digits with respect to their original images (e.g. some of the digit 4 images in ByPE-VAE could be misconstrued as digit 9).

observe the superior generative quality of Hub-VAE compared to Ex-VAE which generates blurred images and does not accurately capture the fine details of the reference image.

2.4 Running Time We compare the running time in seconds of each method for an epoch in Table 6. VAE-Gaussian has the lowest running time. We observe that while Hub-VAE has a higher running time than the compared methods, the time is feasible from a practical standpoint. The bottleneck is the computation of hubs in each epoch, which involves pairwise distance computations. However, approximate nearest neighbor computation can be used to speedup the runtime of Hub-VAE.

Copyright © 2023 by SIAM
Unauthorized reproduction of this article is prohibited

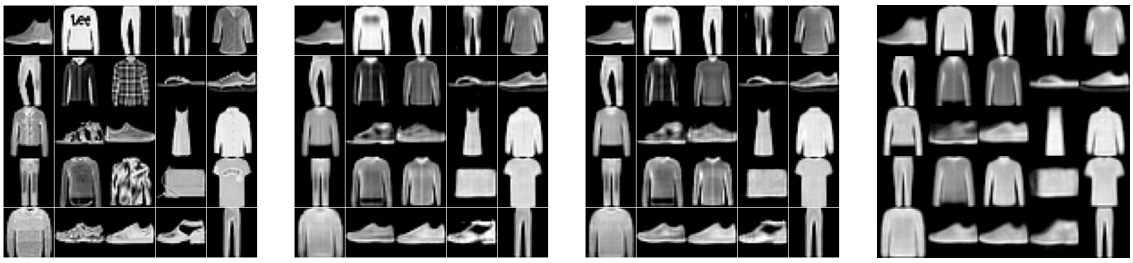

(a) Original Image (b) Hub-VAE (c) Ex-VAE (d) ByPE-VAE

Figure 3: Reconstruction of randomly sampled images of FMNIST from the latent space. (a) shows the original images of the reconstructed data.

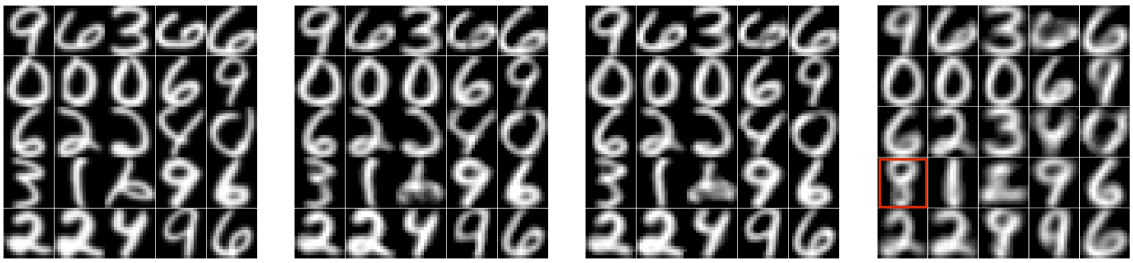

(a) Original Image (b) Hub-VAE (c) Ex-VAE (d) ByPE-VAE

Figure 4: Reconstruction of randomly sampled images of USPS from the latent space. (a) shows the original images of the reconstructed data. Red bounding box on ByPE-VAE shows an incorrect reconstruction.

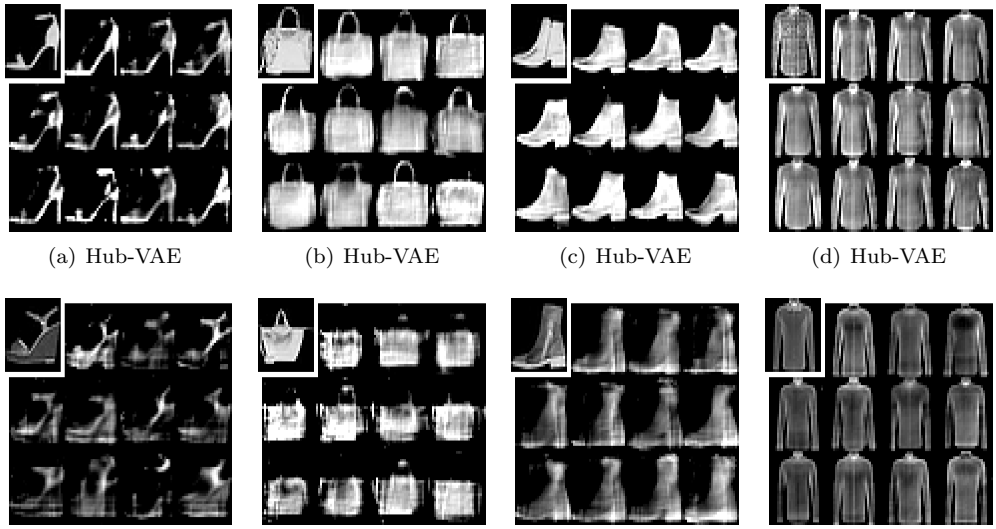

(a) Hub-VAE (b) Hub-VAE (c) Hub-VAE (d) Hub-VAE

(e) Exemplar-VAE (f) Exemplar-VAE (g) Exemplar-VAE (h) Exemplar-VAE

Figure 5: Conditional image generation from chosen classes in FMNIST for (a)-(d) Hub-VAE and (e)-(f) Ex-VAE. The reference images (exemplar) are shown in the inset.

2.5 Hub Characteristics We show the hub characteristics for USPS and Caltech101 in Fig. 6

Copyright © 2023 by SIAM
Unauthorized reproduction of this article is prohibited

Data	VAE-Gaussian	VAE-Vamp	Ex-VAE	ByPE-VAE	Hub-VAE
DMNIST	**5.24**	6.58	7.63	7.01	28.16
FMNIST	**5.46**	6.64	11.12	7.65	33.62
USPS	**1.61**	1.77	1.99	2.06	4.26
Caltech101	**1.45**	1.56	1.75	1.73	4.67
CIFAR-10	**4.7**	5.83	7.93	5.78	28.36

Table 6: Running time (in seconds) per epoch.

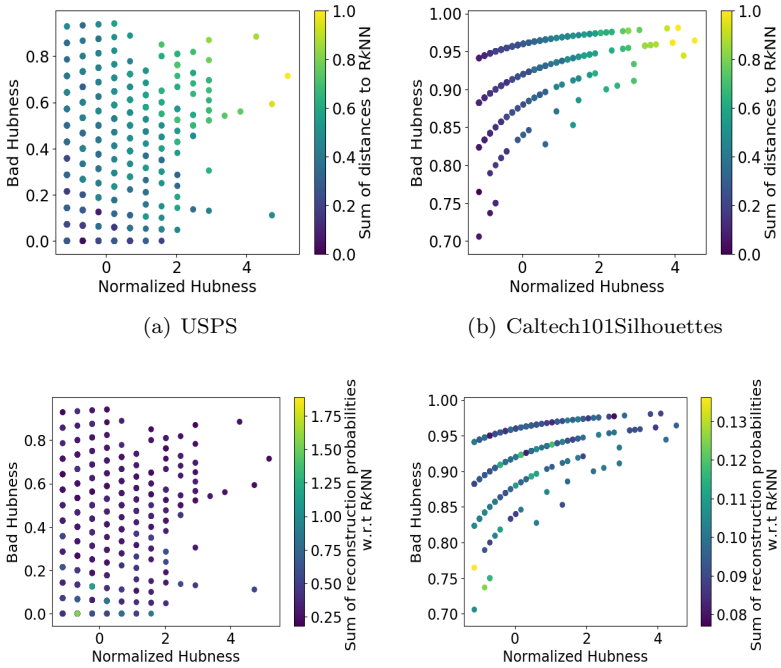

(a) USPS (b) Caltech101Silhouettes

(c) USPS (d) Caltech101Silhouettes

Figure 6: Scatter plots of characteristics of hubs. The x-axis in each sub-plot denotes normalized ($\mu_{N_k} = 0$, $\sigma_{N_k} = 1$) hubness scores. The y-axis denotes bad hubness. The hubs are color-coded by the sum of the pairwise distances to their reverse k-nearest neighbors (RkNN) in plots (a)-(b), and by their reconstruction probabilities w.r.t. the distributions of their RkNN in plots (c)-(d). Hubs with high pairwise distances (top-right quadrant of (a)-(b)) and low reconstruction probabilities (bottom-left quadrant of (c)-(d)) with respect to their RkNN are strong bad hubs.

Copyright © 2023 by SIAM
Unauthorized reproduction of this article is prohibited